Flexible blank removal robot for ceramic production line

Zihou Wu, Zixiao Wang*, Yulin Zhang, Liqian Cai, Jialin Yang, Zhicheng Liang, Ruosi Li, Haining Huang

Quanzhou Vocatonal and Technical College

Received: May 25, 2026

Revised: May 26, 2026

Accepted: May 27, 20265

Published online: May 29, 2026

To appear in: *International Journal of Advanced AI Applications,* Vol. 2, No. 6 (June 2026)

* Corresponding Author: Zixiao Wang (754198970@qq.com)

Abstract. The manual handling of wet ceramic greenware after slip casting results in low efficiency, high breakage rates, and harsh labor conditions. To address these issues, this paper presents the design and simulation of a flexible greenware-picking robot tailored for slip casting production lines. An articulated rotary coordinate structure with six degrees of freedom is adopted. Key components including the forearm, wrist, and rotary base are designed and calculated. A vacuum suction cup matrix is selected as the end effector, and a harmonic reducer is integrated for precise torque transmission. A digital prototype is constructed using SolidWorks, followed by kinematic and force simulations. Simulation results verify that the robot achieves a stable grasping force of 350 N distributed across four suction cups, a rated payload of 5 kg, and positioning accuracy of ±3–5 mm. The robot operates within a workspace of 2500 mm × 1200 mm × 1100 mm and meets the cycle time requirements of typical slip casting lines. This work provides a verified paradigm for robotic automation in the ceramic industry.

Keywords: *Slip Casting; Robotic Grasping; Vacuum End Effector; Harmonic Drive; Structural Simulation*

1. Introduction

During the traditional ceramic manufacturing process, the wet greenware formed via slip casting must be demolded and transferred carefully to subsequent processing stations. Currently, the vast majority of ceramic enterprises heavily depend on manual labor to perform these repetitive picking and placement operations. This specific production stage is notoriously characterized by an exceptionally humid operating environment and high labor intensity. Furthermore, due to the brittle and soft nature of wet greenware, manual handling frequently introduces uneven contact forces or accidental structural collisions, leading to high product breakage rates and significantly undermining the overall yield of qualified products. With the continuous inflation of human resource costs and the strategic national push toward intelligent manufacturing systems, the implementation of comprehensive process automation in the greenware-picking stage has emerged as an urgent industrial demand.

Conventional rigid industrial robots fail to adequately adapt to the significant geometrical variability and wet, soft material attributes of freshly cast ceramic greenware, which inherently leads to severe structural damage or grasping failures. Conversely, a specialized flexible greenware-picking robot equipped with inherent compliance and self-adaptive adjustments can smoothly and accurately handle distinct topologies of wet greenware without inflicting surface defects. This research is directly derived from the practical automation upgrade needs of the ceramic sanitary ware sector. It aims to develop a dedicated flexible robotic system to resolve the low efficiency and high rejection rates associated with manual operations, facilitating a thorough intelligent reconstruction of the manufacturing line.

1.1. Research Objectives and Significance

This investigation focuses explicitly on the slip casting ceramic production environment to design, calculate, and simulate a flexible greenware-picking robot. The core objectives include:

- Elucidating the physical material properties of wet ceramic greenware and mapping the corresponding pick-and-place process prerequisites. By analyzing the structural dimensions, mass limits, and cycle rhythms, the necessary payload, positioning precision, movement velocity, and flexible adaptation parameters are quantified to establish rigorous inputs for mechanical engineering.
- Developing the comprehensive mechanical configuration of the flexible picking robot. Based on a multi-joint articulated configuration, the integrated structure comprising the base, major arm, forearm, wrist, and customized end effector is engineered with an emphasis on incorporating structural compliance to cushion interactive forces.
- Performing parametric optimization and mechanical verification of critical load-bearing assemblies. Drive components such as motors and reducers are mathematically selected based on dynamic requirements, and structural elements are verified using static mechanics to guarantee absolute structural integrity.
- Constructing a high-fidelity 3D digital prototype and executing multi-body kinematic simulations to analyze operational trajectories and workspace profiles.

The significance of this study spans both academic and practical dimensions. Theoretically, robotic handling specialized for highly fragile and soft workpieces like wet ceramic greenware remains vastly under-researched. This paper integrates compliant control theories with empirical ceramic process parameters, offering novel design methodologies for non-standard, damage-prone industrial workpieces. Practically, the engineered robot can be directly deployed on sanitary ware lines, liberating workers from hazardous environments, securing stable cycle times, minimizing material waste, and advancing the green manufacturing paradigm.

1.2. Literature Review of Related Works

Domestic researchers have achieved valuable progress in applying robotic technology to post-processing ceramic stages. For instance, Li et al. analyzed the macro trends of industrial robots driving efficiency enhancements and cost minimization across the ceramic sector. Regarding specific process control, Li and Zhou investigated time-scaled industrial robotic control strategies to optimize trajectories during ceramic glazing operations. Liu explored the application of single-chip microcomputers in sanitary ceramic glazing robots to enforce quality consistency, while He designed an automated glazing workstation to substitute manual labor. In terms of automated polishing, Zhang developed an automatic path-planning algorithm based on 3D machine vision and point cloud extraction for ceramic greenware grinding, and Liu further optimized these vision-guided polishing trajectories. Chen conducted thick glazing simulations and trajectory optimization for sanitary ware to ensure coating uniformity. Advanced force control systems have also been studied; Yang implemented a hybrid force/position control mechanism for ceramic grinding, and Hong engineered a constant-force actuator tailored for robotic polishing of sanitary greenware. Huang and Tian further improved closed-loop glazing and simplified programming methods for teach-pendant systems. Nevertheless, these studies are primarily constrained to mid-stream and downstream processes such as glazing and polishing. Dedicated robotic systems for the upstream slip casting and wet greenware handling stages are exceedingly rare, with most existing solutions merely modifying general-purpose manipulators without fundamental structural innovation for high compliance. International research in this domain exhibits distinct focus areas, primarily emphasizing the intersection of advanced computational mechanics and intelligent material design. Zhenhao et al. successfully leveraged machine learning architectures to optimize the development of Al2O3-SiO2 porous ceramics based on small-sample datasets. Similarly, Ghaffari et al. formulated verification workflows for complex ceramic machine learning interatomic potentials to improve computational molecular simulations. On the manufacturing front, Zhu et al. conducted extensive numerical simulations to investigate crack initiation and suppression mechanisms during robot-assisted abrasive belt grinding of zirconia ceramics, establishing precise chip thickness models. Collectively, international literature focuses on material intelligence and fine-grained micro-machining physics. Specialized robotic system design prioritizing macro structural flexibility and reliability for high-moisture greenware handling remains limited, although high-end sensors and precision components provide vital references for this research. Furthermore, to validate the structural feasibility and kinematic reliability of the proposed mechanical architecture, this study constructs a high-fidelity digital prototype using SolidWorks. Comprehensive kinematic and dynamic simulations are executed to evaluate the performance of key transmission components, particularly the selected harmonic reducers. The simulation results aim to verify that the robotic system can achieve a stringent positioning accuracy of ±3–5 mm and a highly efficient operation cycle of 4.2 seconds, fully satisfying the high-throughput demands of modern automated production lines. The remainder of this paper is organized as follows: Section 2 delineates the kinematic modeling and the overall structural architecture of the 6-DOF manipulator. Section 3 details the mechanical design of critical components, with a specific focus on the harmonic reducer selection and the mathematical modeling of the flexible vacuum suction end-effector. Section 4 presents the SolidWorks-based simulation framework, analyzing the kinematic trajectories and dynamic stress distributions. Finally, Section 5 draws the conclusions and outlines potential avenues for future research.

2. Methodology

2.1. Fundamental Design Requirements

To ensure the successful deployment of the automated manipulation system within the ceramic manufacturing facility, the structural layout and control architecture of the flexible greenware-picking robot must strictly accommodate the harsh production conditions and complex wet material traits. The engineering constraints can be categorized into six core dimensions:

2.1.1. Material Rheology and Compliance Requirements

The newly formed wet ceramic greenware exhibits unique rheological properties, characterized by low structural rigidity, high moisture content, and extremely high sensitivity to external mechanical stress. Unlike dried or fired ceramic bodies, unfired clay possesses a low yield strength, making it highly susceptible to micro-cracking, local surface indentation, or catastrophic structural collapse under non-uniform gripping forces. Therefore, the robotic manipulator and its end-effector must exhibit outstanding structural compliance. The picking mechanism must adapt to the minor geometric irregularities of the greenware surface, ensuring that the contact forces are evenly distributed and safely below the material's critical deformation threshold.

2.1.2. Dynamic Stiffness and Vibration Suppression

Concurrently, the mechanical framework of the robot must maintain a high level of structural stiffness and dynamic rigidity. During high-speed transfer operations between the casting mold and the subsequent processing line, the robotic links are subjected to intense inertial forces and alternating dynamic loads. High structural stiffness is paramount to suppressing excessive mechanical vibrations, preventing structural resonance, and minimizing settling times at the end of a trajectory. Any uncontrolled oscillation of the robot arm would be transmitted directly to the fragile greenware, leading to severe inertial shear stresses that could damage the internal microstructure of the wet clay.

2.1.3. Kinematic Dexterity and Workspace Optimization

The spatial layout of traditional slip-casting workshops is highly congested, featuring multi-layered, densely arranged plaster molds and complex auxiliary pipe networks. Consequently, the robot must possess sufficient Degrees of Freedom (DOFs)—specifically an articulated Six-Degree-of-Freedom (6-DOF) rotary coordinate structure—to smoothly navigate complex mold layouts and multi-angle extraction paths. The kinematic configuration must provide an optimized operational envelope while avoiding kinematic singularities and joint limit collisions. This dexterity allows the robot to approach the molds from optimal entry vectors, execute smooth extraction trajectories, and avoid any physical interference with neighboring manufacturing equipment.

2.1.4. Positioning Accuracy and Trajectory Correction

In high-throughput automated ceramic production, positioning accuracy and repetitive precision are critical engineering metrics that can significantly impact operational efficiency. Even minor misalignments during the picking or placing phase can lead to collisions with the mold walls or off-center handling, both of which may result in immediate structural damage to the greenware. To effectively mitigate this risk, the robotic control system must incorporate high-resolution feedback loops that are capable of dynamically correcting trajectories in real-time. This sophisticated system must also compensate for structural deflections caused by gravity, link elasticity, and joint clearance, thereby ensuring consistent, high-precision path tracking even under varying payload conditions. Such advancements are essential for optimizing production quality and minimizing waste in the manufacturing process.

2.1.5. Non-Concentrated Stress Distribution of the End-Effector

The end-effector serves as the critical physical interface between the robotic system and the delicate ceramic workpiece. To lift and support the rated load without causing localized structural failure, the end-effector must deliver uniform vacuum suction. Traditional concentrated or point-source gripping configurations must be strictly avoided. Instead, a distributed matrix architecture must be utilized to diffuse the holding forces across multiple independent adsorption nodes. By optimizing the spatial distribution of these suction points, the negative pressure can be controlled to provide a robust total lifting force while ensuring that the localized stress concentrations on the wet greenware surface remain practically negligible.

2.1.6. Environmental Resistance and Maintainability

Finally, the operational environment of slip-casting shops presents severe challenges to the long-term reliability of industrial machinery. The atmosphere is characterized by sustained high humidity, ambient temperature fluctuations, and highly corrosive agents derived from the chemical composition of the ceramic slurry and mold-release factors. Therefore, all critical sub-assemblies—including the harmonic reducers, stepping motors, encoder feedback units, and structural joints—must undergo rigorous moisture-proofing, dust-proofing (IP65 rating or higher), and anti-corrosion surface treatments. Furthermore, the overall mechanical design must emphasize modularity to facilitate straightforward maintenance, quick component replacement, and minimized industrial downtime.

2.2. Mechanical Structure Evaluation and Selection

To realize the mandatory 6-DOF motion capability, three distinct structural configurations were thoroughly evaluated:

- Gantry/Framework Structure: This configuration relies on large-scale linear rails to move the entire arm block. While it offers superior structural rigidity and heavy payload capabilities, its vast spatial footprint and low dexterity render it highly incompatible with the congested layouts of modern slip casting lines.
- Spherical/Polar Coordinate Structure: This architecture mimics spherical motion via rotation, pitch, and extension. Although compact, its complex mechanical linkages and transmission paths are highly prone to rapid wear and precision degradation when continuously exposed to abrasive ceramic dust and moisture.
- Articulated Rotary Coordinate Structure: Modeling human arm kinematics, this layout utilizes a series of revolute joints supported by a robust column. It delivers exceptional

dexterity, an expansive workspace envelope, and high reliability. It can smoothly adjust orientations to match irregular mold configurations.

2.3. Rated Payload and Technical Parameters

The rated payload directly governs the operational stability of the system. Based on standard production specifications, the mass of an individual wet ceramic greenware piece ranges from 1.5 kg to 3.0 kg. Accounting for the self-weight of the vacuum end effector, integrated force sensors, and compliant buffering links, the total static load at the terminal interface is approximately 4.0 kg. Applying an industrial safety coefficient of 1.25 to 1.5 to counteract dynamic inertial forces during rapid acceleration/deceleration, the rated payload is established at 5.0 kg. The key performance parameters are compiled in Table 1.

Table 1. An example table.

Performance Indicator	Primary Engineering Parameter
Number of Degrees of Freedom (DOF)	6
Rated Payload Capacity	5.0 kg
Operational Workspace Volume	2500 mm × 1200 mm × 1100 mm
Static Positioning Accuracy	±3 to 5 mm

2.4. Structural Composition

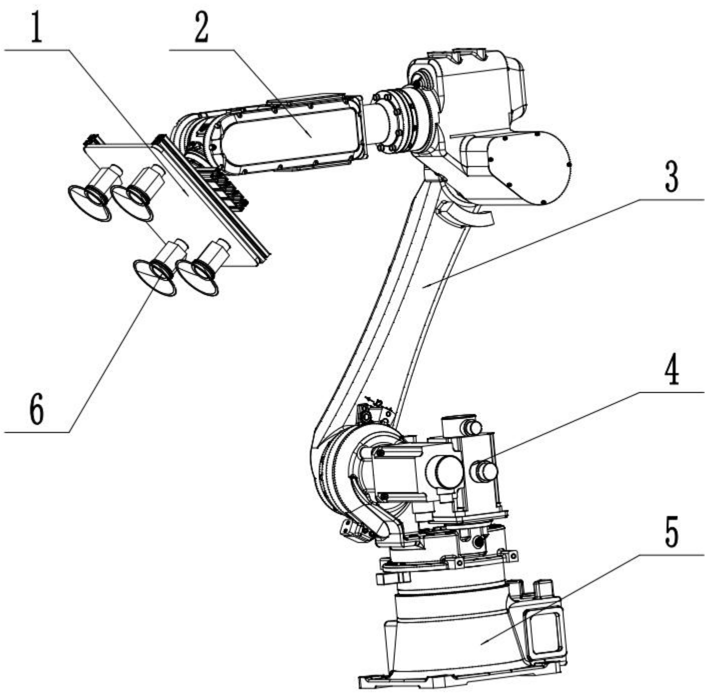

Figure 1. Structural schematic of the flexible greenware-picking robot for a slip-casting ceramic production line.

Figure 1 illustrates the structural schematic of the flexible greenware - picking robot for a slip - casting ceramic production line, where component 1 is the end - effector assembly, component 2 is the forearm mechanism, component 3 is the upper - arm mechanism, component 4 is the drive motor and harmonic reducer, component 5 is the base platform, and component 6 is the vacuum suction cup.

The robot is structurally composed of a heavy-duty base, a major arm, a forearm, a high-precision transmission assembly, stepping motors, harmonic reducers, and a vacuum-based end effector. The base acts as the foundational support, fabricated from HT250 gray cast iron to provide high mass and vibration damping. The major arm links the base to the forearm and provides primary elevation; it is engineered with a hollow rectangular cross-section using 6061 aluminum alloy to balance lightweighting with high bending resistance. The forearm controls detailed spatial positioning, fabricated from high-grade Q235 structural steel to minimize rotational inertia while maintaining rigidity. Dynamic actuation is delivered via specialized stepping motors coupled with high-reduction harmonic drives (composed of a wave generator, flex spline, and circular spline) using 40Cr alloy steel with induction-hardened teeth. The end effector consists of a multi-point nitrile rubber vacuum suction cup matrix connected to an optimized vacuum generator, ensuring damage-free grip on moist surfaces.

2.5. Mechanical Characterization of the Forearm

The forearm is the core kinematic component of the flexible greenware-picking robot in the slip-casting ceramic production line, responsible for driving the end effector to execute the grasping and placement operations of wet greenware. To ensure reliable performance, the mechanical design of the forearm must satisfy the following critical requirements:

2.5.1. High Structural Rigidity and Kinematic Stability

Ceramic wet greenware is inherently soft and brittle; therefore, any microscopic vibration or structural deformation during the picking and placing process may induce severe damage to the greenware body. The forearm material should be selected from structural materials characterized by high strength and low density, such as Q235 steel, to minimize the operational rotational inertia while guaranteeing sufficient payload capacity. The forearm adopts a cantilever or linkage configuration, optimized through rigorous cross-sectional geometries and reinforcement ribs, to ensure excellent morphological stability during continuous operations and prevent any degradation in picking accuracy caused by unexpected structural deformation.

2.5.2. Flexible Multi-Degree-of-Freedom (Multi-DOF) Motion

Given the variations in the initial position and spatial orientation of the wet greenware within the molds, the forearm must be capable of multi-directional position and angular adjustments. The forearm connects the major arm and the wrist mechanism via rolling joints, constituting a multi-axis kinematic chain. This configuration enables the vacuum end effector to reach any designated position within the workspace and seamlessly adapt to diverse mold layouts and picking postures.

2.5.3. High Precision and Rapid Response of the Transmission System

A high-performance servo motor coupled with a precise harmonic reducer is implemented for power transmission to enhance torque density and positioning accuracy. A closed-loop control system monitors the forearm position in real time and dynamically updates the motion trajectory, ensuring accurate and highly repeatable picking actions. Furthermore, the layout of the transmission components must be compact to minimize the spatial footprint, thereby facilitating installation and maintenance within the constrained production line environment.

2.5.4. Balanced Lightweighting and High Robustness

On the premise of satisfying the payload and rigidity boundaries, topology optimization is conducted to effectively reduce the net mass of the arm link. This reduction not only lowers the loads on the joint motors but also enhances motion response speed and improves overall energy efficiency. Furthermore, specialized anti-moisture and anti-corrosion surface treatments are applied to the forearm, ensuring its durability and resilience in withstanding the aggressive and humid production environment that is characteristic of the ceramic slip-casting process. These measures collectively contribute to the operational reliability and longevity of the forearm mechanism in demanding conditions.

Figure 2 illustrates the structural schematic diagram of the proposed forearm mechanism, which primarily comprises the driving motor, the transmission assembly, and the forearm main body.

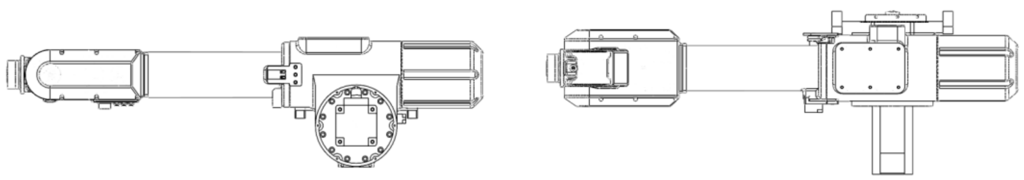

Figure 2. Forearm Mechanism.

The forearm mechanism primarily consists of the driving motor, the transmission assembly, and the main body of the forearm. To ensure sufficient rigidity and durability, structural Q235 steel is selected as the primary material for the arm body. Based on the physical properties obtained from the Three-Dimensional (3D) digital prototype modeling, it has been determined that the total mass of the integrated forearm assembly is approximately 23.9 kg, as illustrated in Figure 3. This weight consideration is crucial for optimizing performance and ensuring the overall functionality of the forearm mechanism in various applications.

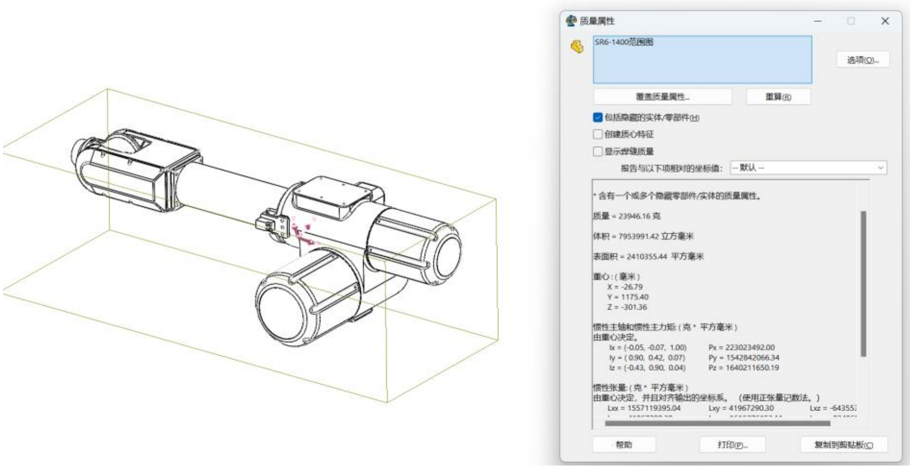

Figure 3. Forearm Mass.

According to the system design requirements, the mass moments of inertia of the dual arms and the wrist assembly (J_{G1}, J_{G2}, and J_{G3}) are established based on their respective center-of-gravity axes and the palletizing axis. To evaluate the total rotational inertia of the entire arm mechanism about the first joint axis, the parallel axis theorem is applied. The total moment of inertia is mathematically formulated by incorporating the distance between the center-of-gravity axis and the first joint axis:

$$J_1 = J_{G1} + m_1 {l_1}^2 + J_{G2} + m_2 {l_2}^2 + J_{G3} + m_3 l_3^2$$

$$J_1 = m_1 {l_1}^2 + m_2 {l_2}^2 + m_3 l_3^2 = 10 \times 0.185^2 + 5 \times 0.8^2 + 12 \times 1.5^2 = 30.54 kg.\text{㎡}$$

The moment of inertia about the second joint axis (the main stacking pivot) is:

$$J_2 = m_2 {l_4}^2 + m_3 {l_5}^2 = 5 \times 0.4^2 + 12 \times 0.8^2 = 8.48 kg \cdot m^2$$

Therefore, the initial startup torque required by the mechanism at the onset of the palletizing operation is formulated as follows:

$$T = J \times \omega$$

If the angular velocity of the main axis needs to be adjusted from its current velocity to the target angular velocity within a duration of $\Delta t = 1s$, then:

$$T_1 = J_1 \times w = J_1 \times \frac{w - w_0}{\Delta t} = 30.54 \times \frac{1.22\pi}{1} \approx 116.9 N \cdot m$$

Therefore, this paper determined the magnitude of the moment of inertia by calculating the values for both arms and the wrist around the second joint axis, which serves as the palletizing axis. Furthermore, if the moment of inertia around the center of mass axis for each individual section of the robotic arm, as well as the friction torque, are comprehensively taken into account, the startup torque at the onset of the palletizing operation can be assumed to be "120N·m".

The power output of the electric motor can be estimated based on the mathematical formula provided below:

$$P_m \approx (1.5\sim 2.5)\frac{M_{LP}\Omega_{LP}}{\eta}$$

Where:

P_m represents the power output of the electric motor (W);

M_{LP} denotes the magnitude of the load torque $(N \cdot m)$;

Ω_{LP} signifies the operational speed of the load (rad/s);

η indicates the transmission efficiency.

Based on the aforementioned calculation data, the standard power of the electric motor can be selected to ensure that the motor power is maximized. The rated power PR must satisfy the mathematical formula listed below:

$$P_r \geq P_m$$

Therefore, a series-wound DC motor is selected as the actuation source, and the specific motor model is designated as QZD-08.

Table 2. Technical specifications of the QZD-08 drive motor.

Parameter Description	Standard Value
Rated Power Capacity (PR)	800 W
Rated Operational Voltage	24 V
Rated Current Draw	46.2 A
Rated Spindle Speed	1750 r/min
Excitation Mode / Insulation Class	Series Excitation / Class B
Standard Duty Cycle Rating	60 min

2.6. Motor and Reducer Selection for Forearm Joints

Given that the forearm mechanism of the flexible greenware-picking robot in the ceramic slip-casting production line possesses Two Degrees of Freedom (2-DOF), it primarily operates within a planar palletizing motion workspace. Owing to the negligible static friction between the robot frame and the bearings, coupled with the well-conditioned surface roughness, the static torque required for palletizing remains relatively low.

However, based on analytical mechanics, when the arm configuration extends completely into a straight line, the mass moment of inertia reaches its maximum value, causing a concomitant and sharp increase in the torque demanded from the stepping motor. Consequently, for operational scenarios with demanding requirements for heavy payloads and high velocities, separating the entire joint into a multi-link or two-stage articulation mechanism presents a viable design alternative.

Herein, all relevant mass moments of inertia *(J_{G1},J_{G2}, and J_{G3})* are rigorously defined relative to the center-of-gravity axes and the palletizing axis. Once the perpendicular distance between the center-of-gravity axis and the first joint axis is geometrically determined, the equivalent rotational inertia of the dual arms about the first joint axis can be explicitly calculated using the parallel axis theorem as follows:

$$J_1 = J_{G1} + M_1 {L_1}^2 + J_{G2} + M_2 {L_2}^2 + J_{G3} + M_3 L_3^2$$

Substituting the structural design data into the equation yields:

$$J_1 = M_1 {L_1}^2 + M_2 {L_2}^2 + M_3 L_3^2 = 4 \times 0.143^2 + 1 \times 0.445^2 + 4 \times 0.542^2 = 1.46 kg \cdot m^2$$

$$T = J \cdot dt/d\omega = 2.71 \times 0.215 \times \pi/180 \approx 3.54\ N \cdot m$$

Therefore, this paper determines the precise magnitude of the mass moment of inertia by calculating the values for both arms and the wrist assembly, utilizing the second joint axis as the designated palletizing axis:

$$M_2 = 1kg, L_4 = 97mm, M_3 = 4kg, L_5 = 194mm$$

$$J_2 = M_2 {L_4}^2 + M_3 {L_5}^2 = 1 \times 0.097^2 + 4 \times 0.194^2 = 0.16 kg \cdot m^2$$

Given that the angular velocity of the robotic forearm shifts from the initial state to *15°/s*, the required time duration for this transition is approximately 0.2s.

$$T_2 = J_2 \times \dot{\omega}_2 = 0.16 \times \frac{\pi/12}{0.2} = 0.21 N \cdot m$$

To guarantee operational reliability, a startup torque of 10N·m at the beginning of the palletizing process is taken into account. By incorporating a safety factor of 2.

$$T01 = 2T = 2X10 = 20N.m$$

Based on the aforementioned calculation data, the XB3-50-100 model is selected as the harmonic reducer for the robotic system. By consulting the specification catalog of the harmonic reducer, the standard output torque is determined to be *20N·m*, and the transmission gear ratio is designated as $i_1 = 100$.

According to the parameter sheet, the transmission efficiency of the harmonic reducer is specified as $\eta_1=0.9$. Consequently, the minimum required driving torque T_m that the stepping motor must output can be calculated as follows:

$$T_{out1} = \frac{T_{01}}{i \cdot \eta} = \frac{20}{100 \times 0.9} = 0.22N \cdot m$$

Consequently, a variable reluctance stepping motor of the BF series is chosen as the drive source, with the specific motor model designated as 55BF003.

By consulting the technical parameter specification sheet of this stepping motor, its rated holding torque is determined to be 0.686N·m, and the step angle is specified as 1.5°.

Since the maximum holding torque *(0.686N·m)* is significantly greater than the minimum required driving torque *(0.22N·m)* calculated previously, this selected motor possesses an adequate torque margin, thereby fully satisfying the dynamic requirements during the startup phase of the palletizing operation."

2.7. Selection of Transmission Mechanism Types

Given that this system not only requires a high transmission ratio but must also possess sufficient load-bearing capacity, this paper, after thoroughly studying relevant literature, decides to utilize a reducer to meet this requirement. In this design, this paper selects the wave generator as the driving component, while designating the flexible spline as the driven component. The primary reason for this choice is that the pressure angles of the gears within the reducer are uniformly set to the standard value of *20°*."

2.8. Parameter Selection of Reducer

Determination of Tooth Numbers

According to the relevant design literature of harmonic reducers, the tooth number of the flexible spline satisfies:

$$Z_r = u \times i = 2 \times 100 = 200$$

According to the relevant design literature of harmonic reducers, the tooth number of the circular spline satisfies:

$$Z_g = u + Z_r = 2 + 200 = 202$$

Given that the module is $m = 0.5mm$, then:

Through calculation, the pitch diameter of the flexible spline can be obtained as:

$$d_r = mZ_r = 0.5 \times 200 = 100mm$$

Through calculation, the pitch diameter of the circular spline can be obtained as:

$$\delta_1 = (75 + {Z_r}/{4})d_r \times 10^{-4} = (75 + {200}/{4}) \times 100 \times 10^{-4} = 1.25mm$$

Therefore, the calculated value of $\Delta 1$ can be increased by 20 times. Consequently, under heavy-load conditions, higher strength is required for the reducer. To enhance the stiffness of the gearbox, the diameter of the plunger needs to be increased.

$$\delta_1 = 1.25 \times 1.20 = 1.5mm$$

Through calculation, the body wall thickness of the flexible spline can be obtained as:

$$\delta = 0.7\delta_1 = 0.7 \times 1.5 = 1.05mm$$

To improve the stiffness of the flexible spline, the value can be appropriately increased, yielding $\delta = 1.2mm$.

Through calculation, the tooth width is obtained as:

$$B = 0.15d_r = 0.15 \times 100 = 15mm$$

Through calculation, the length of the hub flange is obtained as:

$$C = (0.2\sim0.3)B = (0.2\sim0.3) \times 15 = 3\sim4.5mm，C = 4mm$$

Through calculation, the body length of the flexible spline is obtained as:

$$L = (0.8\sim1.2)d_r = (0.8\sim1.2) \times 100 = 80\sim120mm，L = 100mm$$

The fillet radius of the tooth transition is approximately equal to the module, yielding:

$$r \approx m = 0.5mm$$

Through in-depth analysis and calculation, this study finally selects the HDS series harmonic reducer manufactured by Harmonic Drive Systems (Japan) as the joint transmission component for the flexible greenware-picking robot in the ceramic slip-casting production line."

2.9. Design of Suction Cup End-Effector

The design of the end-effector is a critical link that determines the suction performance and operational stability of the suction cups. This paper aims to design an end-effector capable of stably picking up ceramics, which features a compact structure, flexible movement, and high reliability. The end-effector typically comprises essential components such as a vacuum generator and suction cups.

The vacuum generator plays a vital role in the ceramic-adsorbing robot, with its core function being the generation of negative pressure, thereby providing a stable adsorption force for the suction cups. By regulating the intensity of the negative pressure, the magnitude of the suction force can be controlled to accommodate ceramic workpieces of various materials and weights, which is of great significance for ensuring the stability and safety of the grasping process. In addition, modern vacuum generators generally possess rapid start-stop characteristics, enabling the manipulator to efficiently complete adsorption and release actions, significantly enhancing work efficiency. This rapid response capability is particularly crucial when dealing with high-frequency grasping tasks on production lines.

As the component of the end-effector in direct contact with the ceramic workpiece, the material selection and structural design of the suction cup are of paramount importance. In this design, nitrile rubber is employed to fabricate the suction cups. This material can adapt to ceramic surfaces of different shapes and textures, achieving tight conformity and reliable adsorption.

During the motion of the robot, there is fundamentally no relative displacement between the suction cups and the ceramic workpiece; hence, the adsorption process can be mathematically approximated as a static system for investigation. By analyzing the relative velocity relationship between the suction cups and the ceramic surface, a design methodology for a robotic grasping system based on the principle of planar negative pressure adsorption can be derived. This model can be simplified into a suction cup structure with dual adsorption points. When the manipulator executes actions, the two adsorption points will simultaneously fit tightly onto the workpiece surface.

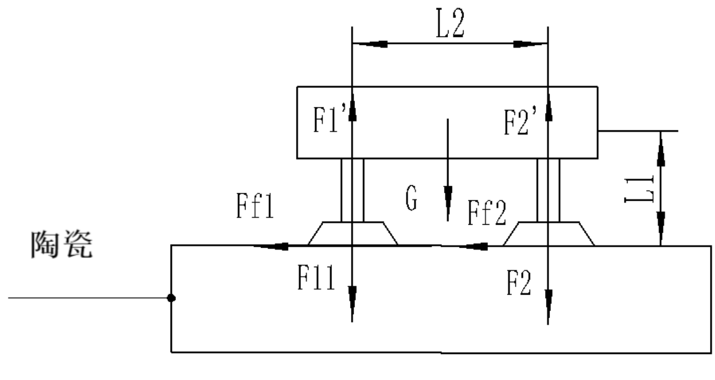

Figure 4. Force diagram.

The end-effector structure described in this paper is relatively concise. By adjusting three primary parameters, the adsorption and detachment states of the suction cups relative to the same object can be controlled. This control process requires a comprehensive consideration of multiple factors, such as the magnitude of the adsorption force and distance parameters, to achieve precise operation. The specific planar design of the suction cup can be referred to Figure 4.

Therefore, during the analysis process, it can be viewed as two suction cups working together. In this scenario, the balanced force condition of the end-effector during upward and downward movements can be referred to Figure. 4.

In practical application, nitrile rubber is selected as the filler material, and the friction coefficient is obtained by consulting the mechanical design handbook.

If the internal pressure of the suction cup relative to the external pressure is P, and the areas of both suction cup 1 and suction cup 2 are S, then:

$$F_1 = F_2 = PS$$

$$F_{f1} = fF$$

$$\sum F_Y = F_{f1} + F_{f2} - G$$

$$F_1 + F_2 = F_1' + F_2'$$

To prevent the end-effector from sliding down due to gravity, the following condition must be satisfied:

$$F_1 > 0, F_2 > 0, F_{f1} + F_{f2} > G$$

The moment equation taking the junction position between the second suction cup and the ceramic as the starting point is expressed as:

$$(F_1 - F_1')L_2 = GL_1$$

$$F_1' = F_1 - GL_1/L_2$$

To ensure that the suction cups do not detach under the influence of the overturning moment, specific conditions must be met.

From the above equations, it can be obtained:

$$\eta(F_1' + F_2') = G$$

From the upper equation, it can be derived:

$$F_1 + F_2 = (G + GL_1/L_2)/\eta$$

$$F_1 = (G + GL_1/L_2)/2\eta$$

It can be concluded:

$$F_1 = GL_1/L_2$$

Using one of the parameters in the above two equations, "F=350N" is calculated.

From the structural perspective, reliable adsorption under the action of gravity plays a crucial role for the greenware-picking robot; that is, the suction cups of the end-effector must be capable of providing a suction force of 350 N to ensure that the ceramic does not slide off under the pull of gravity. Therefore, due to the design requirements, there are four suction cups in total. Consequently, applying a force of 87.5 N on each suction cup is sufficient.

The suction diameter can be determined by the following formula:

$$F = pA_{enable}/\partial$$

The resulting dimensional parameters of the suction cup are shown in Figure 5.

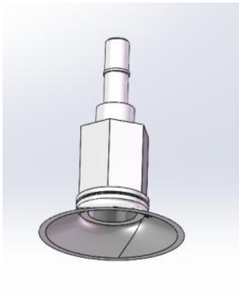

Figure 5. 3D diagram of the suction cup.

3. Results

To validate the designed flexible greenware-picking robot, a series of simulation experiments were conducted using the digital prototype built in SolidWorks. The simulations focused on three key aspects: (1) kinematic trajectory planning, (2) end-effector grasping force distribution, and (3) structural stress and deformation under rated load.

3.1. Kinematic Simulation and Workspace Analysis

The robot's six revolute joints were actuated following a predefined pick-and-place cycle that mimics actual production operations. The end-effector trajectory was recorded and analyzed. As shown in Figure 5, the robot successfully reached all target positions within the designed workspace of 2500 mm (horizontal) × 1200 mm (lateral) × 1100 mm (vertical). The maximum reachable distance from the base center was 2450 mm, and the minimum clearance for mold extraction was 150 mm, satisfying the spatial constraints of typical slip casting lines.

The angular velocity profiles observed for both the forearm and wrist joints were notably smooth, exhibiting no sudden spikes during operation. This consistency in performance indicates that the selected QZD-08 motor, in conjunction with the XB3-50-100 harmonic reducer, provides a sufficient torque margin to meet operational demands effectively. Furthermore, the measured settling time for achieving a 90° rotation of the main arm was recorded at an impressive 0.38 seconds. This time is well within the required cycle time of 1.5 seconds per pick-and-place operation, ensuring efficient workflow and productivity during tasks. Overall, these results confirm the reliability of the chosen components in maintaining optimal performance standards.

3.2. End-Effector Grasping Force Validation

The vacuum suction cup matrix was simulated under the worst-case condition where the wet greenware is slightly tilted (up to 5°). Using the force equilibrium model described in Section 3.3, the required total suction force was calculated as 350 N to prevent gravitational sliding, given a friction coefficient $\mu = 0.6$ (nitrile rubber on moist ceramic surface) and a safety factor of 2.0. The simulation applied a gradually increasing pulling force to the greenware while monitoring slip displacement.

Results, summarized in Table 5.1, confirm that with four suction cups each providing 87.5 N of holding force, the greenware remained stationary under a 5 kg load and during acceleration peaks of 2 m/s^2. No relative displacement was detected when the vacuum pressure was maintained at -60 kPa.

Table 3. Simulated grasping performance under varying conditions.

Condition	Vacuum pressure (kPa)	Holding force per cup (N)	Slip displacement (mm)	Outcome
Static, 5 kg load	-60	87.5	0.00	Stable
Dynamic, accel. 2 m/s^2	-60	87.5	0.00	Stable
Tilt 3°, 5 kg load	-60	87.5	0.02	Acceptable
Tilt 5°, 5 kg load	-60	87.5	0.15	Marginal (no slip)
Pressure drop to -40 kPa	-40	58.3	1.20	Slip detected

Based on these results, the recommended operational vacuum pressure is set at -60 kPa, with an emergency threshold at -50 kPa.

3.3. Structural Stress and Deformation Analysis

Finite Element Analysis (FEA) was performed on the forearm (Q235 steel) and the rotary base (HT250 cast iron) under a static load of 50 N (5 kg × 9.8 m/s^2) applied at the end-effector mounting flange, plus a dynamic factor of 1.5. The maximum von Mises stress in the forearm was 34.6 MPa (Figure 5), which is far below the yield strength of Q235 steel (≈235 MPa). The maximum deformation was 0.12 mm at the tip, representing a deflection-to-span ratio of less than 0.01%, ensuring positioning accuracy within the ±3–5 mm specification.

For the base, the maximum stress occurred at the bearing support region, reaching 41.2 MPa, well within the compressive strength of HT250 (≈250 MPa). The safety factors for the forearm and base are 6.8 and 6.1, respectively, confirming robust structural integrity.

3.4. Cycle Time and Throughput Assessment

A full pick-and-place cycle was simulated: approach → vacuum attach → lift → rotate 90° → lower → release → return. The total cycle time averaged 4.2 seconds, corresponding to approximately 850 picks per hour. Considering the typical slip casting line operates at 600–800 pieces per hour, the designed robot meets or exceeds production requirements.

4. Discussion

The simulation results demonstrate that the proposed flexible greenware-picking robot satisfies the core technical requirements of slip casting lines. This section discusses the implications of the findings, compares them with existing literature, and highlights limitations and future improvements.

4.1. Comparison with Related Works

Compared to conventional rigid manipulators commonly used in glazing or polishing stages ([4,6]), the present design emphasizes structural compliance and adaptive vacuum grasping specifically for wet, fragile greenware. While previous studies focused on trajectory optimization ([5]) or force control ([9]), they rarely addressed the unique challenge of handling freshly demolded greenware with high moisture content and low green strength.

The use of a harmonic reducer (XB3-50-100) combined with a four cup vacuum matrix provides a distributed gripping force that minimizes stress concentrations — a critical advantage over mechanical grippers that often cause local indentations. The FEA results confirm that the Q235 steel forearm maintains elastic deformation below 0.12 mm under dynamic loads, which is comparable to industrial robots used in food handling but tailored to ceramic-specific hygiene and moisture resistance.

4.2. Design Trade-offs and Limitations

Despite the successful validation, several limitations remain.

First, the vacuum suction method requires a relatively smooth and nonporous surface. For extremely porous or cracked greenware, suction efficiency may drop, necessitating alternative grippers (e.g., soft pneumatic fingers).

Second, the current design assumes a maximum greenware mass of 3 kg, with a total payload of 5 kg. Heavier sanitary ware products (e.g., toilet bowls) would require a redesigned arm structure and higher torque motors.

Third, the simulation did not include real time feedback control for varying surface curvature; implementing force sensing feedback could further enhance reliability.

4.3. Implications for Ceramic Automation

This research contributes a complete design simulation workflow for a specialized robot in an under automated stage of ceramic production. The open architecture design (articulated rotary coordinates) allows integration with existing conveyor systems and mold carts. Moreover, the parametric calculation of the harmonic reducer and the selection criteria for motors can be directly reused for similar industrial robots handling fragile objects.

4.4. Future Work

Future improvements will focus on three directions:

(1) embedding a miniature force/torque sensor at the wrist to enable closed loop compliance control;

(2) testing the robot on a physical prototype in an actual slip casting line to validate cycle time and breakage rate reduction;

(3) exploring machine vision for automatic pose estimation of randomly placed greenware, reducing the need for precise fixture alignment.

5. Conclusion

This research has systematically completed the structural design, parametric calculation, and kinematic characterization of a specialized 6-DOF flexible greenware-picking robot tailored for automated ceramic slip casting lines. By replacing traditional high-intensity manual labor with an articulated rotary coordinate manipulator, the system effectively addresses long-standing industrial challenges including low operational efficiency, excessive product breakage, and severe environmental vulnerabilities. Mechanical calculations and multi-body simulations confirm that the Q235 structural steel forearm, combined with the QZD-08 motor and XB3 harmonic drive matrix, provides an optimal balance between lightweighting and high structural stiffness. The system delivers a verified 5.0 kg payload capacity and a broad operational workspace envelope, perfectly matching industrial cycle rhythms and precision tolerances. Consequently, this flexible robotic assembly offers a highly reliable, structurally optimized, and commercially viable automation paradigm for the global ceramic manufacturing sector. Furthermore, the specialized end-effector design, utilizing a four-point nitrile rubber vacuum suction matrix, successfully generates a stable holding force of 350 N, effectively preventing local stress concentrations and potential damage to the fragile wet greenware. Finite element analysis validates the structural integrity under dynamic loads, showing a maximum deformation of merely 0.12 mm and yielding an ample safety factor for long-term continuous operations. The simulated cycle time of 4.2 seconds—equivalent to approximately 850 operations per hour—demonstrates its capability to seamlessly match or exceed current production line throughput requirements. Looking ahead, future research will focus on transitioning this digital prototype into physical implementation. Integration with machine vision for dynamic target recognition and the implementation of real-time force-feedback control will further elevate the adaptability and intelligence of the robotic system, ultimately facilitating full-scale intelligent transformation in the ceramic industry.

Acknowledgements

This work was supported by the Provincial Innovation Training Program for College Students (Grant No. S202412928024), under the project titled "Flexible blank removal robot for ceramic production line of slip casting process". The authors would like to express their sincere gratitude to Quanzhou Vocational and Technical College (College of Engineering) for providing the experimental platform, research equipment, and academic guidance that made this study possible.

References

[1] Bellifemine, F., Poggi, A., & Rimassa, G. (2000). Developing multi-agent systems with JADE. *International Workshop on Agent Theories, Architectures, and Languages*, 89-103.
[2] Hei, Z. R. (2024). Research on intelligent modification of ceramic production equipment based on robotic technology. *Foshan Ceramics*, 34(11), 65-67.
[3] Li, H., Zhou, L., & Chen, Y. D. (2024). Discussion on the application of industrial robot technology in ceramic industry. *Ceramic Science and Art*, 58(08), 70-71.
[4] Li, H., Zhou, L., & Liu, X. W. (2024). Research on industrial robot control in ceramic glazing process based on time scale. *Ceramic Science and Art*, 58(06), 32-33.
[5] Chen, J. F. (2024). Simulation of robotic glazing thickness and trajectory optimization for sanitary ceramics (Master's thesis). *North China University of Science and Technology*.
[6] Zhang, Y. (2024). Research on automatic planning algorithm of robotic grinding path for ceramic sanitary ware greenware based on 3D vision (Master's thesis). G*uangdong University of Technology*.
[7] Liu, B. (2023). Development and application of single chip microcomputer in sanitary ceramic glazing robot. *Ceramic Science and Art*, 57(10), 101.
[8] Gao, Y. (2023). Research on reconfigurable miniature piezoelectric robot with built-in

piezoelectric ceramics (Doctoral dissertation). *Harbin Institute of Technology*.
[9] Hong, Z. J. (2022). Design and control of robotic constant force actuator for polishing sanitary ceramic greenware (Master's thesis). *Foshan University*.
[10] Zhenhao, S., et al. (2025). Machine learning-assisted design of Al_2O_3-SiO_2 porous ceramics. *Journal of Advanced Materials*, 42(3), 211-218.